Atmos. Chem. Phys. Discuss., 11, 2025–2055, 2011
www.atmos-chem-phys-discuss.net/11/2025/2011/
doi:10.5194/acpd-11-2025-2011

Atmospheric Chemistry and Physics Discussions

Secondary Organic Aerosol formation from phenolic compounds in the absence of NO_x

S. Nakao[1,2], C. Clark[1,2], P. Tang[1,2], K. Sato[2,*], and D. Cocker III[1,2]

[1]University of California, Riverside, Department of Chemical and Environmental Engineering, Riverside, California, USA
[2]College of Engineering – Center for Environmental Research and Technology (CE-CERT), Riverside, California, USA
[*]currently at: National Institute for Environmental Studies, Japan

Received: 4 December 2010 – Accepted: 9 December 2010 – Published: 20 January 2011

Correspondence to: D. Cocker III (dcocker@engr.ucr.edu)

Published by Copernicus Publications on behalf of the European Geosciences Union.

Abstract

SOA formation from benzene, toluene, *m*-xylene, and their corresponding phenolic compounds were investigated using the UCR/CE-CERT Environmental Chamber to evaluate the importance of phenolic compounds as intermediate species in aromatic SOA formation. SOA formation yield measurements coupled to gas-phase yield measurements indicate that approximately 20% of the SOA of benzene, toluene, and *m*-xylene could be ascribed to the phenolic route. The SOA densities tend to be initially as high as approximately 1.8 g/cm^3 and eventually reach the range of 1.3–1.4 g/cm^3. The final SOA density was found to be independent of elemental ratio (O/C) indicating that applying constant density (e.g., 1.4 g/cm^3) to SOA formed from different aromatic compounds is a reasonable approximation. Results from a novel on-line PILS-ToF (Particle-into-Liquid Sampler coupled with Agilent Time-of-Flight) are reported. Major signals observed by the on-line/off-line ToF include species consistent with bicyclic hydroperoxides. To the authors' best knowledge, this is the first possible detection of bicyclic hydroperoxides in aromatic SOA.

1 Introduction

Secondary organic aerosol (SOA) is formed from oxidative processing of volatile organic compounds in the atmosphere. SOA has been suggested to contribute to climate change (IPCC, 2007; Kanakidou et al., 2005), adverse human health effects (Davidson et al., 2005; Pope and Dockery, 2006), and a reduction in visibility (Eldering and Cass, 1996). Previous researchers have estimated approximately 70% of organic aerosols are secondary in nature (Hallquist et al., 2009 and references therein). Aromatic hydrocarbons comprise ~20% of nonmethane hydrocarbons in the urban atmosphere and are considered to be one of the major precursors to urban SOA (Calvert et al., 2002).

A number of studies have investigated gas-phase photooxidation of aromatic hydrocarbons (e.g., Calvert et al., 2002; Olariu et al., 2002; Volkamer et al., 2002; Takekawa

ACPD
11, 2025–2055, 2011

et al., 2003; Johnson et al., 2004, 2005; Coeur-Tourneur et al., 2006; Arey et al., 2009). Previously identified first generation products of aromatic compound photooxidation explain approximately 50% of carbon balance (Calvert et al., 2002). Although multi-generational reactions have been suggested to contributed to aromatic SOA formation (Hurley et al., 2001; Ng et al., 2007; Sato et al., 2007), the extent of the contribution from the second or further reaction products to SOA is poorly understood.

Phenolic compounds are one of the major first generation products of OH reaction with aromatic hydrocarbons (Calvert et al., 2002). Previous studies suggested the major gas-phase reaction products from OH reaction of phenolics are dihydroxy compounds (e.g., 80% catechol formation from phenol, Olariu et al., 2002). However, the mechanisms of SOA formation from phenolic compounds are highly uncertain. In addition, since phenolic compounds are significant products in wood smoke (Schauer et al., 2001; Simoneit, 1999; Hawthorne et al., 1989; Hawthorne et al., 1992), the reaction mechanism of phenolic compounds leading to SOA formation is of a great interest (Chang and Thompson, 2010; Grosjean, 1984; Sun et al., 2010; Iinuma et al., 2010; Henry et al., 2008; Coeur-Tourneur et al., 2010a, b).

NO_x concentration impacts SOA formation from aromatic hydrocarbons (Song et al., 2005, 2007; Ng et al., 2007). SOA formation under low NO_x conditions has been observed to be higher, which is generally ascribed to increased contribution of organic hydroperoxides (ROOH) (Song et al., 2007; Ng et al., 2007). This study focuses on low NO_x conditions where ROOH species are expected to strongly contribute to SOA formation. It evaluates the importance of phenolic compounds as intermediate species of aromatic SOA formation.

ACPD
11, 2025–2055, 2011

2 Experimental

2.1 Smog chamber

Most of the experiments were conducted in the UC Riverside/CE-CERT environmental chamber described in detail in Carter et al. (2005). In short, this facility consists of dual 90 m^3 Teflon® reactors suspended by rigid frames in a temperature controlled enclosure (27 ± 1 °C) continuously flushed with purified air. The top frames are slowly lowered during the experiments to maintain a slight positive differential pressure (0.03″ H_2O) between the reactors and enclosure to minimize dilution and possible contamination of the reactors. 272 115 W Sylvania 350 black lights are used as the light source for all the experiments reported herein.

Some of the results of dimethylphenols (DMPs) were acquired in the CE-CERT mezzanine chamber. The CE-CERT mezzanine chamber is a 2.5 m × 3 m × 7.8 m enclosure covered with reflective aluminum sheet and is illuminated with 170 of 40 W blacklights with peak intensity at 350 nm (SYLVANIA, 350 BL) with the NO_2 photolysis rate of 0.6 min^{-1}. Within this enclosure is a 12 m^3 volume 2 mil FEP Teflon® film reactor. A minimum of 1 m space between the reactor surface and blacklights avoids excessive heating at the surface of the film. Six fans are used to mix the air inside the enclosure with room air to minimize heating in the enclosure. Prior to each experiment, the bag is flushed by pure air (Aadco 737 series air purification system (Cleves, Ohio)) until the background particle concentration is below detection (<0.2 cm^{-3}).

2.2 Gas and particle analysis

The Agilent 6890 Gas Chromatograph – Flame Ionization Detector was used to measure concentrations of reactants and products. All phenolic compounds were analyzed by a GC equipped with a thermal desorption system (CDS analytical, ACEM9305, Sorbent Tube MX062171 packed with Tenax-TA/Carbopack/Carbosieve S111). Aromatic hydrocarbon measurements were calibrated using a dilute gas

ACPD
11, 2025–2055, 2011

cylinder (SCOTT-MARIN, Inc.) or by introducing known amount of liquid hydrocarbons into the reactor. Calibration for phenolic compounds was performed by impregnation of the glass cartridges with known quantities of phenolic compounds in acetonitrile. The Ionicon Proton Transfer Reaction – Mass Spectromer (PTR-MS) was also used to observe gas phase compounds with higher proton affinity than water.

Particle size distribution between 28 nm and 700 nm was monitored by a custom built Scanning Mobility Particle Sizer (SMPS) similar to that described by Cocker et al. (2001). Particle effective density was measured with an Aerosol Particle Mass Analyzer (APM, Kanomax) (Ehara et al., 1996) and SMPS in series. The APM is located upstream of the SMPS for improved time resolution and sensitivity (S/N) over the more common configuration of Differential Mobility Analyzer (DMA) – APM (Khalizov et al., 2009; McMurry et al., 2002; Xue et al., 2009). A detailed description of the APM-SMPS system and data algorithms are described elsewhere (Malloy et al., 2009).

The HR-ToF-AMS (DeCarlo et al., 2006) was operated in high resolution W mode. Elemental analysis (EA) was used to determine the atomic ratio (O/C) of non-refractory organic aerosols (Aiken et al., 2008).

The Agilent 6210 Accurate-Mass Time-of-Flight equipped with multimode ionization source for electrospray and atmospheric pressure chemical ionization (ESI/APCI-ToF) is used to obtain accurate mass of analytes. Soft ionization by ESI and/or APCI provides lower fragmentation of the analytes compared to electron impact (EI) used for the HR-ToF-AMS or other conventional GC-MS techniques. Mass accuracy is routinely calibrated by standard compounds before analysis and in most cases mass accuracy of less than 5 ppm is achieved. Occasionally higher mass errors (~30 ppm) were observed during sample analysis, which resulted in a consistent shift of mass throughout the mass range of the instrument. Since the extent of the shift can be inferred from repeatedly observed ions (e.g., pyruvid acid, reference mixture), formulas were carefully assigned based on tendency of shift and repeat experiments. Filter samples were collected onto Teflo® filters (2 µm, 47 mm, PALL Life Sciences) at 25 L/min for 1~4 h. After collection, filters were stored in a freezer until extraction. Extractions were achieved

ACPD
11, 2025–2055, 2011

done by sonicating the filter in 5mL of acetonitrile. The extract volume was reduced under a gentle stream of N_2 until near dryness and reconstituted by 300 µL of acetonitrile/water/acetic acid (50/50/0.1 v). A: Water (0.1 v% acetic acid) and B: acetonitrile were used for LC eluents (B 50%, 0.5 mL/min). Mixed mode ionization (simultaneous APCI and ESI) was used with vaporizer temperature 200 °C, nebulizer pressure 40 psig, corona current 2 µA, fragmentor voltage 100 V. All the Agilent ToF data was acquired in negative polarity mode.

A Particle-Into-Liquid-Sampler (PILS) (Weber et al., 2001; Orsini et al., 2003) was interfaced with the Time-of-Flight to provide a on-line accurate mass analysis of water soluble organic compounds (Bateman et al., 2010). The PILS-ToF system will be described in detail in an upcoming publication (Clark et al., 2011). The negative ESI was used as the ionization method (similar condition as the filter analysis without the corona current).

2.3 Chamber experiments

The experimental test matrix is summarized in Table 2. A known volume of high purity liquid aromatic hydrocarbon (All purchased from Sigma-Aldrich: ≥99% or ≥99.5%, except 2,4-DMP ≥98%) was injected through a heated glass injection manifold system and flushed into the chamber with pure N_2. Since phenolic compounds are less volatile than hydrocarbons typically used for chamber experiments, injection into the chambers were carefully performed using a heated oven (50~80 °C) through heated transfer line maintained at a temperature higher than oven. The glass manifold inside the oven was packed with glass wool to increase the mass transfer surface area. Since reasonable agreement between the calculated concentration of phenolics (based on injected amount) and observed concentrations were confirmed, loss of phenolics in transfer line and to the wall was assumed to be negligible. H_2O_2 50 wt% solution was injected through the same oven system. Since the H_2O_2 solution did not spread through glass wool, the glass wool was processed with an acid/base bath and cleaned by water and acetone which enabled the H_2O_2 solution to spread. Initial H_2O_2 concentration was not

ACPD
11, 2025–2055, 2011

measured, but is estimated to be 1∼5 ppm based on amount injected and hydrocarbon decay rate. To investigate the role of organic peroxides, additional high NO experiments were also performed and the chemical composition of SOA was compared to low NO_x condition. Initial ratio of approximately 50/50/500 ppb for phenolic/methyl nitrite/NO was used to ensure that excess NO was present to suppress $RO_2 + HO_2$ reaction.

3 Results and discussion

3.1 SOA formation

SOA yield (Y) is defined as the mass of aerosol formed (wall-loss-corrected) (M_o) divided by mass of hydrocarbon reacted (ΔHC)

$$Y = \frac{M_o}{\Delta \mathrm{HC}} \tag{1}$$

Its dependence on aerosol mass loading has been traditionally parameterized by as shown below: Odum et al. (1996)

$$Y = \sum Y_i = M_o \sum_i \frac{\alpha_i K_i}{1 + M_o K_i} \tag{2}$$

where α_i is the mass-based stoichiometric coefficient for the reaction generating product i, K_i is the partitioning coefficient of product i. Equations (1) and (2) were applied for the SOA yields obtained (Fig. 1). Particle density of 1.4 g/cm^3 was used. 2,4-DMP had the highest SOA formation potential of the three DMP isomers, with a SOA yield approximately twice as high as the other DMP isomers. SOA yield from phenol was higher than benzene.

SOA from aromatic hydrocarbons formed in low NO_x condition was previously reported to be effectively non-volatile (Ng et al., 2007), in which case SOA yield would be independent of particle mass concentration (flat SOA yield curves). However, for

ACPD
11, 2025–2055, 2011

benzene, *o*-/*m*-cresol, and possibly DMPs, the SOA yield was observed to be slightly dependent on particle concentration. Therefore, in this study, constant SOA yield was not assumed and a one product model fit was applied to perform calculation of the contribution of phenolic route in the following section of the contribution of phenolic route.

3.2 Formation of phenolic compounds from aromatic hydrocarbons

The formation yields of phenolics from aromatics were obtained. An example for *o*-cresol and *m*/*p*-cresol formation from toluene is shown in Fig. 2. The cresol formation yields from toluene were calculated from measured cresol by correcting for the further reaction of cresols with OH. Equations in Atkinson et al. (1982) and rate constants from Calvert et al. (2002) were used for the correction. Phenol, cresols, and DMPs formation yields are in reasonable agreement with previous studies(Table 2) (Smith et al., 1998; Berndt and Boge, 2006; Volkamer et al., 2002; Atkinson, 1989; Klotz et al., 1998; Smith et al., 1999; Atkinson et al., 1991).

3.3 Contribution of phenolic route

Contributions of the phenolic route to aromatic SOA formation in the low NO_x system were estimated by combining SOA yield measurement (Fig. 1), phenolic yields, and consumption of phenolics (e.g., Fig. 2). The amount of phenolics (as products) reacted is calculated as the gap between the observed concentration of phenolic compounds and the concentration corrected for the secondary reaction. Phenolic route SOA is calculated by multiplying reacted phenolics and their SOA yield at appropriate mass loading using the phenolic SOA yield curves in Fig. 1. SOA yields from cresol isomers (*o*-, *m*-, and *p*-) were assumed to be the same (Henry et al., 2008). The ratio of 2,4-DMP and 2,6-DMP produced from OH reaction of *m*-xylene was assumed to be the same as that reported by Smith et al. (1999). Formation of 3,5-DMP is assumed to be insignificant (Smith et al., 1999). Contribution of the phenolic route in the no

ACPD
11, 2025–2055, 2011

NO_x system is summarized in Table 3. The contribution was approximately 20% for benzene, toluene, and *m*-xylene.

3.4 SOA density and elemental ratio

Real-time SOA density measured by the APM-SMPS is shown in Fig. 3. The SOA densities were observed to be initially high (~1.8 g/cm^3), which could be due to high density of nucleating species. The final SOA densities were in the range of 1.3–1.4 g/cm^3, in reasonable agreement with previous studies (Ng et al., 2007; Sato et al., 2010). Although Bahreini et al. (2005) observed weak correlation between effective density and relative contribution of *m/z* 44 signal to total organic signal of AMS, the final SOA densities were found to be independent of elemental composition of SOA (Fig. 4). Therefore a constant SOA density (1.4 g/cm^3) is applied to all the experiments in this study.

3.5 Gas phase analysis

The PTR-MS detected several gas phase products with higher *m/z* than reactants. A *m/z* 171 was detected in *m*-xylene experiments, but not in DMPs experiments (Fig. 5). A *m/z* 171 is consistent with a bicyclic ketone (Wyche et al., 2009; Birdsall et al., 2010). The absence in DMP experiments is consistent with its formation mechanism- DMPs should form analog products with additional -OH (not detected). *m/z* 139 was detected in the cresol experiments. Also *m/z* 153, additional 14 (-CH_2), was confirmed in DMPs and *m*-xylene experiments. These products are tentatively assigned as dihydroxybenzaldehydes (Fig. 6, molecular weight 138) and dihydroxytolualdehydes (molecular weight 152), which can be formed by OH addition to form dihydroxy compounds (Olariu et al., 2002) and subsequent H abstraction of the methyl substitute.

3.6 Particle chemical composition

Chemical composition of SOA was analyzed by off-line filter analysis. Mass spectrum obtained by ESI/APCI-ToF is shown in Fig. 7. High mass accuracy measurements

ACPD
11, 2025–2055, 2011

enabled determination of empirical formula. Some of the ions in the three spectrums are consistent with -CH_2 shift, such as $C_6H_8O_6$ and $C_6H_8O_7$ in phenol SOA (Fig. 7a′). $C_6H_8O_6$ is consistent with bicyclic hydroperoxides formed from phenol. The presence of bicyclic species as gas-phase products of OH reaction with aromatic hydrocarbons has been suggested experimentally and theoretically (Glowacki et al., 2009; Andino et al., 1996; Huang et al., 2008; Wyche et al., 2009; Birdsall et al., 2010). Johnson et al. (2004, 2005) predicted bicyclic hydroperoxides as one of the predominant aerosol species from aromatic hydrocarbons. To the authors' best knowledge, bicyclic species in particle phase have not been observed previously.

The presence of peroxides was investigated by conducting experiments under excess NO. In excess NO condition, the (bicyclic) peroxy radicals rapidly react with NO to form the alkoxy radical, which is suggested to undergo decomposition (Calvert et al., 2002; Atkinson, 2000). The ESI/APCI-ToF mass spectrum of SOA in high NO condition is shown in Fig. 8. $C_6H_8O_6$ (*m/z* 175) and $C_6H_8O_7$(*m/z* 191) observed in Fig. 7a were not significantly observed. The highest signal of *m/z* 154 is consistent with nitrocatechol which is consistent with the previous model prediction (Johnson et al., 2005; Kelly et al., 2010) that the major product from OH reaction with toluene under high NO_x condition include methylnitrocatechol formed from methylcatechols, and observation by Iinuma et al. (2010) that significant methylnitrocatechol was formed from *m*-cresol in high NO_x condition.

The absence of *m/z* 175 and *m/z* 191 in Fig. 8 suggests that peroxy radicals are key precursors for these compounds (*m/z* 175, 191). A possible formation pathway for $C_6H_8O_6$ formation is shown in Fig. 9.

3.7 PILS-ToF

Mass spectrum obtained by PILS-ESI-ToF of SOA formed from OH reaction with phenol, catechol, and *o*-cresol are shown in Fig. 10.

Major signals observed in filter analysis were also observed by the PILS-ToF such as *m/z* 175 and 191 in phenol SOA mass spectrum (Fig. 10a). Since the PILS-ToF

ACPD
11, 2025–2055, 2011

was operated without a denuder upstream, water soluble gas-phase compounds can potentially be collected by the PILS system. The highest signal in Fig. 10a (mass spectrum when SOA was highest), *m/z* 109 is catechol ($C_6H_6O_2$), which is consistent with previous gas-phase studies (Olariu et al., 2002). From *o*-cresol, methylcatechol (*m/z* 123) was observed. Although further reaction mechanisms of catechol species is highly uncertain, a series of signals consistent with -OH addition to catechol was observed ($C_6H_6O_2$, $C_6H_6O_3$, $C_6H_6O_4$, $C_6H_6O_5$), which could imply successive addition of -OH group to the aromatic ring.

3.8 Implication

The potential role of bicyclic hydroperoxides as a key intermediate species of phenolic SOA formation could be useful for modeling studies to predict aromatic SOA formation. Conventional techniques such as GC-MS can not observe this species, due to weak bonding of the peroxides. The quantification of bicyclic hydroperoxides may improve the current poor understanding of aromatic SOA composition (typically up to 10%). Further structural studies of phenolic SOA using soft ionization techniques and, for example, ion trap mass spectrometry is recommended.

4 Conclusions

Significance of phenolic compounds as intermediate species of aromatic SOA and possible SOA formation mechanism in the absence of NO_x was investigated using the UCR/CE-CERT Environmental Chamber. SOA formation yield measurements coupled to gas-phase yield measurements indicate that approximately 20% of the SOA of benzene, toluene, and *m*-xylene could be ascribed to the phenolic route. Initial SOA densities were as high as approximately 1.8 g/cm^3 and eventually reached the range of 1.3–1.4 g/cm^3, independent of elemental ratio (O/C) of SOA. Major signals from online PILS-ToF and off-line filter analysis agreed, with some additional possible water

ACPD
11, 2025–2055, 2011

soluble gas phase products observed by PILS-ToF such as catechol. Major signals observed by ESI/APCI-ToF included species consistent with bicyclic hydroperoxides. To the authors' best knowledge, this is the first detection of bicyclic hydroperoxides in aromatic SOA.

Acknowledgements. We gratefully acknowledge funding support from University of California Transportation Center, W. M. Keck Foundation, National Science Foundation (ATM-0449778 and ATM-0901282), California Air Resources Board, and University of California, Riverside, Department of Chemical and Environmental Engineering. We also acknowledge Kurt Bumiller and Charles Bufalino for experimental setup, William P. L. Carter for helpful discussions, Norman Ho and Mary Kacarab for chemical analysis.

References

Aiken, A. C., DeCarlo, P. F., Kroll, J. H., Worsnop, D. R., Huffman, J. A., Docherty, K., Ulbrich, I., Mohr, C., Kimmenl, J. R., Sun, Y., et al.: O/C and OM/OC ratios of primary, secondary, and ambient organic aerosols with High-Resolution Time-of-Flight Aerosol Mass Spectrometry, Environ. Sci. Technol., 42, 4487–4485, 2008.

Andino, J. M., Smith, J. N., Flagan, R. C., Goddard, W. A., and Seinfeld, J. H.: Mechanism of atmospheric photooxidation of aromatics: A theoretical study, J. Phys. Chem., 100, 10967–10980, 1996.

Arey, J., Obermeyer, G., Aschmann, S. M., Chattopadhyay, S., Cusick, R. D., and Atkinson, R.: Dicarbonyl products of the OH radical-initiated reaction of a series of aromatics hydrocarbons, Environ. Sci. Technol., 43, 683–689, 2009.

Atkinson, R.: Kinetics and mechanisms of the gas-phase reactions of the hydroxyl radical with organic compounds, J. Phys. Chem. Ref. Data, Monograph 1, 1989.

Atkinson, R.: Atmospheric chemistry of VOCs and NOx, Atmos. Environ., 34, 2063–2101, 2000.

Atkinson, R., Aschmann, S. M., Carter, W. P. L., Winer, A. M., and Pitts, J. N.: Alkyl nitrate formation from the NOx - air photooxications of C2-C8 n-alkanes, J. Phys. Chem., 86, 4563–4569, 1982.

Atkinson, R., Aschmann, S. M., and Arey, J.: Formation of ring-retaining products from the OH radical-initiated reactions of o-, m-, and p-xylene, Int. J. Chem. Kinet., 23, 77–97, 1991.
Bahreini, R., Keywood, M. D., Ng, N. L., Varutbangkul, V., Gao, H., Flagan, R. C., Seinfeld, J. H., Worsnop, D. R., and Jimenez, J. L.: Measurements of secondary organic aerosol form oxidation of cycloalkenes, terpenes, and m-xylene using an aerodyne Aerosol Mass Spectrometer, Environ. Sci. Technol., 39, 5674–5688, 2005.
Bateman, A. P., Nizkorodov, S. A., Laskin, J., and Laskin, A.: High-resolution electospray ionization mass spectrometry analysis of water-soluble organic aerosol collected with a particle into liquid sampler, Anal. Chem., 82, 8010–8016, 2010.
Berndt, T. and Boge, O.: Formation of phenol and carbonyls from the atmospheric reaction of OH radicals with benzene, Phys. Chem. Chem. Phys., 8, 1205–1214, 2006.
Birdsall, A. W., Andreoni, J. F., and Elrod, M. J.: Investigation of the role of bicyclic peroxy radicals in the oxidation mechanism of toluene, J. Phys. Chem., 114, 10655–10663, 2010.
Calvert, J. G., Atkinson, R., Becker, K. H., Kamens, R. M., Seinfeld, J. H., Wallington, T. J., and Yarwood, G.: The mechanism of atmospheric oxidation of aromatics hydrocarbons, Oxford University Prss, 2002.
Carter, W. P. L., Cocker, D. R., Fitz, D. R., Malkina, I. L., Bumiller, K., Sauer, C. G., Pisano, J. T., Bufalino, C., and Song, C.: A new environmental chamber for evaluation of gas-phase chemical mechanisms and secondary aerosol formation, Atmos. Environ., 39, 7768–7788, 2005.
Chang, J. L. and Thompson, A. E.: Characterization of colored products formed during irradiation of aqueous solutions containing H2O2 and phenolic compounds, Atmos. Environ., 44, 541–551, 2010.
Clark, C. C., Nakao, S., Sato, K., Qi, L., Asa-Awuku, A., and Cocker, D. R., III: Chemical Characterization by Particle into Liquid Sampling Directly Coupled to an Accurate Mass Time-of-Flight Mass Spectrometer (PILS-ToF) of Secondary Organic Aerosol (SOA), in preparation, 2011.
Cocker, D. R., Flagan, R. C., and Seinfeld, J. H.: State-of the art chamber facility for studying atmospheric aerosol chemistry, Environ. Sci. Technol., 35, 2594–2601, 2001.
Coeur-Tourneur, C., Henry, F., Janquin, M.-A., and Brutier, L.: Gas-phase reaction of hydroxyl radicals with m-, o- and p-cresol, Int. J. Chem. Kinet., 38, 553–562, 2006.
Coeur-Tourneur, C., Cassez, A., and Wenger, J. C.: Rate coefficients for the gas-phase reaction of hydroxyl radicals with 2-methoxyphenol (Guaiacol) and related compounds, J. Phys.

ACPD
11, 2025–2055, 2011

Chem., 114, 11645–11650, 2010a.
Coeur-Tourneur, C., Foulon, V., and Lareal, M.: Determination of aerosol yields from 3-methylcatechol and 4-methylcatechol ozonolysis in a simulation chamber, Atmos. Environ., 44, 853–857, 2010b.
Davidson, C. I., Phalen, R. F., and Solomon, S.: Airborne particulate matter and human health: A review, Aerosol Sci. Technol., 39, 737–749, 2005.
DeCarlo, P. F., Kimmel, J. R., Trimborn, A. M., Northway, M., Jayne, J. T., Aiken, A. C., Gonin, M., Fuhrer, K., Horvath, T., Docherty, K., Worsnop, D. R., and Jimenez, J. L.: Field-deployable, high-resolution, Time-of-Flight Aerosol Mass Spectrometer, Anal. Chem., 78, 8281–8289, 2006.
Ehara, K., Hagwood, C., and Coakley, K. J.: Novel method to classify aerosol particles according to their mass-to-charge ratio-Aerosol particle mass analyzer, J. Aerosol Sci., 27, 217–234, 1996.
Eldering, A. and Cass, G. R.: Source-oriented model for air pollutant effects on visibility, J. Geophys. Res., 101, 19343–19369, 1996.
Glowacki, D. R., Wang, L., and Pilling, M. J.: Evidence of formation of bicyclic species in the early stages of atmospheric benzene oxidation, J. Phys. Chem. A, 113, 5385–5396, 2009.
Grosjean, D.: Atmospheric reactions of ortho cresol: Gas phase and aerosol products, Atmos. Environ., 18, 1641–1652, 1984.
Hallquist, M., Wenger, J. C., Baltensperger, U., Rudich, Y., Simpson, D., Claeys, M., Dommen, J., Donahue, N. M., George, C., Goldstein, A. H., Hamilton, J. F., Herrmann, H., Hoffmann, T., Iinuma, Y., Jang, M., Jenkin, M. E., Jimenez, J. L., Kiendler-Scharr, A., Maenhaut, W., McFiggans, G., Mentel, Th. F., Monod, A., Prévôt, A. S. H., Seinfeld, J. H., Surratt, J. D., Szmigielski, R., and Wildt, J.: The formation, properties and impact of secondary organic aerosol: current and emerging issues, Atmos. Chem. Phys., 9, 5155–5236, doi:10.5194/acp-9-5155-2009, 2009.
Hawthorne, S. B., Krieger, M. S., Miller, D. J., and Mathiason, M. B.: Collection and quantitation of methoxylated phenol tracers for atmospheric pollution from residential wood stoves, Environ. Sci. Technol., 23, 470–475, 1989.
Hawthorne, S. B., Miller, D. J., Langenfeld, J. J., and Krieger, M. S.: PM-10 high-volume collection and quantitation of semi- and nonvolatile phenols, methoxylated phenols, alkanes, and polycyclilc aromatic hydrocarbons from winter urban air and their relationship to wood smoke emissions, Environ. Sci. Technol., 26, 2251–2262, 1992.

ACPD
11, 2025–2055, 2011

Henry, F., Coeur-Tourneur, C., Ledoux, F., Tomas, A., and Menu, D.: Secondary organic aerosol formation from the gas phase reaction of hydroxyl radicals with m-, o- and p-cresol, Atmos. Environ., 42, 3035–3045, 2008.
Huang, M., Zhang, W., Wang, Z., Hao, L., Zhao, W., Liu, X., Long, B., and Fang, L.: Theoretical investigation on the detailed mechanism of the OH-initiated atmospheric photooxidation of o-xylene, Int. J. Quantum Chem., 108, 954–966, 2008.
Hurley, M. D., Sokolov, O., Wallington, T. J., Takekawa, H., Karasawa, M., and Klotz, B.: Organic aerosol formation during the atmospheric degradation of toluene, Environ. Sci. Technol., 35, 1358–1366, 2001.
Iinuma, Y., Boge, O., Grafe, R., and Herrmann, F.: Methyl-nitrocatechols: Atmospheric tracer compounds for biomass burning secondary organic aerosols, Environ. Sci. Technol., 44, 8453–8459, 2010.
IPCC, Intergovernmental Panel on Climate Change: Climate Change 2007: The Physical Science Basis, Cambridge University Press, UK, 2007.
Johnson, D., Jenkin, M., Wirtz, K., and Martin-Reviejo, M.: Simulating the formation of secondary organic aerosol from the photooxidation of toluene, Environ. Chem., 1, 150–165, 2004.
Johnson, D., Jenkin, M. E., Wirtz, K., and Martin-Reviejo, M.: Simulating the formation of secondary organic aerosol from the photooxidation of aromatics hydrocarbons, Environ. Chem., 2, 35–48, 2005.
Kanakidou, M., Seinfeld, J. H., Pandis, S. N., Barnes, I., Dentener, F. J., Facchini, M. C., Van Dingenen, R., Ervens, B., Nenes, A., Nielsen, C. J., Swietlicki, E., Putaud, J. P., Balkanski, Y., Fuzzi, S., Horth, J., Moortgat, G. K., Winterhalter, R., Myhre, C. E. L., Tsigaridis, K., Vignati, E., Stephanou, E. G., and Wilson, J.: Organic aerosol and global climate modelling: a review, Atmos. Chem. Phys., 5, 1053–1123, doi:10.5194/acp-5-1053-2005, 2005.
Kelly, J. L., Michelangeli, D. V., Makar, P. A., Hastie, D. R., Mozurkewich, M., and Auld, J.: Aerosol speciation and mass prediction from toluene oxidation under high NOx conditions, Atmos. Environ., 44, 361–369, 2010.
Khalizov, A. F., Zhang, R., Zhang, D., Xue, H., Pagels, J., and McMurry, P. H.: Formation of highly hygroscopic soot aerosols upon internal mixing with sulfuric acid vapor, J. Geophys. Res., 114, D05208, doi:10.1029/2008JD010595, 2009.
Klotz, B., Sorensen, S., Barnes, I., Becker, K. H., Etzkorn, T., Volkamer, R., Platt, U., Wirtz, K., and Martin-Reviejo, M.: Atmospheric oxidation of toluene in a large-volume outdoor photore-

ACPD
11, 2025–2055, 2011

actor: In situ determination of ring-retaining product yields, J. Phys. Chem. A, 102, 10289–10299, 1998.
Malloy, Q., Nakao, S., Qi, L., Austin, R. L., Stothers, C., Hagino, H., and Cocker, D. R.: Real-time aerosol density determination utilizing a modified Scanning Mobility Particle Sizer – Aerosol Particle Mass Analyzer system, Aerosol Sci. Technol., 43, 673–678, 2009.
McMurry, P. H., Wang, X. W., Park, K., and Ehara, K.: The relationship between mass and mobility for atmospheric particles: A new technique for measuring particle density, Aerosol Sci. Technol., 36, 227–238, 2002.
Ng, N. L., Kroll, J. H., Chan, A. W. H., Chhabra, P. S., Flagan, R. C., and Seinfeld, J. H.: Secondary organic aerosol formation from m-xylene, toluene, and benzene, Atmos. Chem. Phys., 7, 3909–3922, doi:10.5194/acp-7-3909-2007, 2007.
Odum, J. R., Hoffman, T., Bowman, F., Collins, D., Flagan, R. C., and Seinfeld, J. H.: Gas/particle partitioning and secondary organic aerosol yields, Environ. Sci. Technol., 30, 2580–2585, 1996.
Olariu, R. I., Klotz, B., Barnes, I., Becker, K. H., and Mocanu, R.: FT-IR study of the ring-retaining products from the reaction of OH radicals with phenol, o-, m-, and p-cresol, Atmos. Environ., 36, 3685–3697, 2002.
Orsini, D. A., Ma, Y., Sullivan, A., Sierau, B., Baumann, K., and Weber, R. J.: Refinements to the particle-into-liquid sampler (PILS) for ground and airborne measurements of water soluble aerosol composition, Atmos. Environ., 37, 1243–1259, 2003.
Pope, C. A. and Dockery, D. W.: Health effects of fine particulate air pollution: Lines that connect, J. Air Waste Manage. Assoc., 56, 709–742, 2006.
Sato, K., Hatakeyama, S., and Imamura, T.: Secondary organic aerosol formation during the photooxidation of toluene: NOx dependence of chemical composition, J. Phys. Chem. A, 111, 9796–9808, 2007.
Sato, K., Takami, A., Isozaki, T., Hikida, T., Shimono, A., and Imamura, T.: Mass spectrometric study of secondary organic aerosol formed from the photo-oxidation of aromatic hydrocarbons, Atmos. Environ., 44, 1080–1087, 2010.
Schauer, J. J., Kleeman, M. J., Cass, G. R., and Simoneit, B. R. T.: Measurement of emissions from air pollution sources. 3. C1-C29 organic compounds from fireplace combustion of wood, Environ. Sci. Technol., 35, 1716–1728, 2001.
Simoneit, B. R. T.: A review of biomarker compounds as source indicators and tracers for air pollution, Environ. Sci. Pollut. Res., 6, 159–169, 1999.

ACPD
11, 2025–2055, 2011

Smith, D. F., McIver, C. D., and Kleindienst, T. E.: Primary product distribution from the reaction of hydroxyl radicals with toluene at ppb NOx mixing ratios, J. Atmos. Chem., 30, 209–228, 1998.
Smith, D. F., Kleindienst, T. E., and McIver, C. D.: Primary product distributions from the reaction of OH with m-, p-xylene, 1,2,4- and 1,3,5-trimethylbenzene, J. Atmos. Chem., 34, 339–364, 1999.
Song, C., Na, K., and Cocker, D. R.: Impact of the hydrocarbon to NOx ratio on secondary organic aerosol formation, Environ. Sci. Technol., 39, 3143–3149, 2005.
Song, C., Na, K., Warren, B., Malloy, Q., and Cocker, D. R.: Secondary organic aerosol formation from m-xylene in the absence of NOx, Environ. Sci. Technol., 41, 7409–7416, 2007.
Sun, Y. L., Zhang, Q., Anastasio, C., and Sun, J.: Insights into secondary organic aerosol formed via aqueous-phase reactions of phenolic compounds based on high resolution mass spectrometry, Atmos. Chem. Phys., 10, 4809–4822, doi:10.5194/acp-10-4809-2010, 2010.
Takekawa, H., Minoura, H., and Yamazaki, S.: Temperature dependence of secondary organic aerosol formation by photo-oxidation of hydrocarbons, Atmos. Environ., 37, 3413–3424, 2003.
Volkamer, R., Klotz, B., Barnes, I., Imamura, T., and Washida, N.: OH-initiated oxidation of benzene Part 1. Phenol formation under atmospheric conditions, Phys. Chem. Chem. Phys., 4, 1598–1610, 2002.
Weber, R. J., Orsini, D. A., Daun, Y., Lee, Y.-N., Klotz, P. J., and Brechtel, F.: A particle-into-liquid collector for rapid measurement of aerosol bulk chemical composition, Aerosol Sci. Technol., 35, 718–727, 2001.
Wyche, K. P., Monks, P. S., Ellis, A. M., Cordell, R. L., Parker, A. E., Whyte, C., Metzger, A., Dommen, J., Duplissy, J., Prevot, A. S. H., Baltensperger, U., Rickard, A. R., and Wulfert, F.: Gas phase precursors to anthropogenic secondary organic aerosol: detailed observations of 1,3,5-trimethylbenzene photooxidation, Atmos. Chem. Phys., 9, 635–665, doi:10.5194/acp-9-635-2009, 2009.
Xue, H., Khalizov, A. F., Wang, L., Zheng, J., and Zhang, R.: Effects of coating of dicarboxylic acids on the mass-mobility relationship of soot particles, Environ. Sci. Technol., 43, 2787–2792, 2009.

ACPD
11, 2025–2055, 2011

Table 1. Experimental test matrix (low NO_x).

	Run ID	HC_i, (ppb)	HC_f, (ppb)	ΔHC (μg/m^3)	Mo (μm/cm^3)	SOA yield
	*benzene + H_2O_2*					
	EPA1141A	491	434	182	25	0.19
	EPA1149A	490	429	195	26	0.18
	EPA1161A	1031	929	326	64	0.28
	EPA1161B	528	478	160	21	0.19
	EPA1225A	953	833	383	73	0.27
	EPA1225B	959	882	246	36	0.20
	*phenol + H_2O_2*					
	EPA1206A	51	21	115	35	0.43
	EPA1206B	52	20	122	40	0.45
	EPA1217A	138	49	338	96	0.40
	EPA1217B	76	28	184	51	0.38
	*catechol+ H_2O_2*					
	EPA1293A	71[a]	0	318	89	0.39
	*toluene + H_2O_2*					
	EPA1266A	104	77	100	12	0.17
	EPA1251B	84	59	93	12	0.19
	EPA1141B	85	57	108	15	0.20
	EPA1290B	432	326	397	65	0.23
	*o-cresol+ H_2O_2*					
	EPA1251A	75	27	210	74	0.49
	EPA1252A	54	12	184	52	0.39
	EPA1252B	45	8	166	41	0.35
	EPA1266B	101	41	263	87	0.46
	*m-cresol+ H_2O_2*					
	EPA1255A	67	18	212	41	0.27
	EPA1255B	55	16	174	38	0.31
	*m-xylene + H_2O_2*					
	EPA1244A	124	47	333	57	0.24
	EPA1180B	234	90	621	134	0.30
	EPA1209A	229	77	656	126	0.27
	EPA1209B	177	59	509	95	0.26
	EPA1212A	114	21	401	91	0.32
	EPA1212B	52	6	197	45	0.32
	EPA1248A	315	262	229	16	0.10
	EPA1248B	121	48	318	48	0.21

ACPD
11, 2025–2055, 2011

Table 1. Continued.

	Run ID	HC_i, (ppb)	HC_f, (ppb)	ΔHC (μg/m^3)	Mo (μm/cm^3)	SOA yield
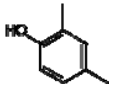	*2,4-DMP + H_2O_2*					
	EPA1238A	83	6	381	199	0.73
	EPA1238B	62	2	293	140	0.67
	mezzanine chamber runs[b]					
	mez100809	68	2.2	327	222	0.95
	mez100909	131	4.9	628	331	0.74
	mez101009	48	1	234	108	0.65
	mez101109	72	2	349	155	0.62
	mez101309	77	1.9	373	197	0.74
	mez102109	66	1	322	162	0.70
	*2,6-DMP + H_2O_2*					
	EPA1240A	98	6	457	134	0.41
	EPA1240B	58	2	278	75	0.38
	mezzanine chamber runs[b]					
	mez081409	64	0	319	79	0.35
	mez081609	66	0	327	86	0.37
	mez081809	67	16	255	24	0.13
	mez100609	64	2.8	305	95	0.44
	mez100709	130	2.7	632	196	0.43
	mez120309	125	0	621	149	0.34
	mez120409	96	0	478	124	0.36
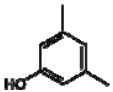	*3,5-DMP + H_2O_2*					
	EPA1243A	90	9	400	83	0.29
	EPA1243B	60	7	262	33	0.17
	mezzanine chamber runs[b]					
	mez051910	72.24	0	359	61	0.24
	mez052010	85.09	0	422	75	0.25
	mez052310	154.1	0	765	148	0.27
	mez060210	160.5	0	797	174	0.31

[a] Initial concentration calculated by amount injected. Injection done with oven temperature ~120 °C.
[b] Initial DMPs concentrations calculated based on injection. Final concentration obtained by the PTR-MS.

ACPD
11, 2025–2055, 2011

Table 2. Phenolic formation yield from OH reaction with benzene, toluene, and *m*-xylene.

	Phenolic formation yield (%)		NO_x (ppm)
	Phenol		
This study	41.3		0
Berndt and Boge (2006)	61 ± 6		0
Volkamer et al. (2002)	53.1 ± 6		0.002-2
	o-Cresol	(*m* + *p*)-Cresol	
This study	15.8	7.3	0
Atkinson et al. (1989)	20.4 ± 2.7	4.8 ± 0.9	0-10
Klotz et al. (1998)	12.0 ± 1.4	5.9 ± 0.9	0.003–0.3
Smith et al. (1998)	12.3 ± 0.6	5.6 ± 0.4	0.10–0.42
	(2,4 + 2,6 + 3,5)-DMP		
This study*	8.2 ± 1.3		0
Smith et al. (1999)	10.9 ± 0.5		0.157–1.081
Atkinson et al. (1991)	21.0 ± 5.6		0–10
Noda et al. (2009)	14.1 ± 2.6		0.01–0.1

* Acquired in mezzanine chamber using PTR-MS.

ACPD
11, 2025–2055, 2011

Table 3. Estimated contribution of phenolic route to benzene, toluene, and *m*-xylene SOA.

	Benzene	Toluene	*m*-Xylene
Phenolicroute (%)	23.5 ± 4.7*	15.8 ± 3.8*	16.9 ± 3.4 ($n = 4$)

* Error estimated based on repeated m-xylene experiments and phenolic route calculations.

ACPD
11, 2025–2055, 2011

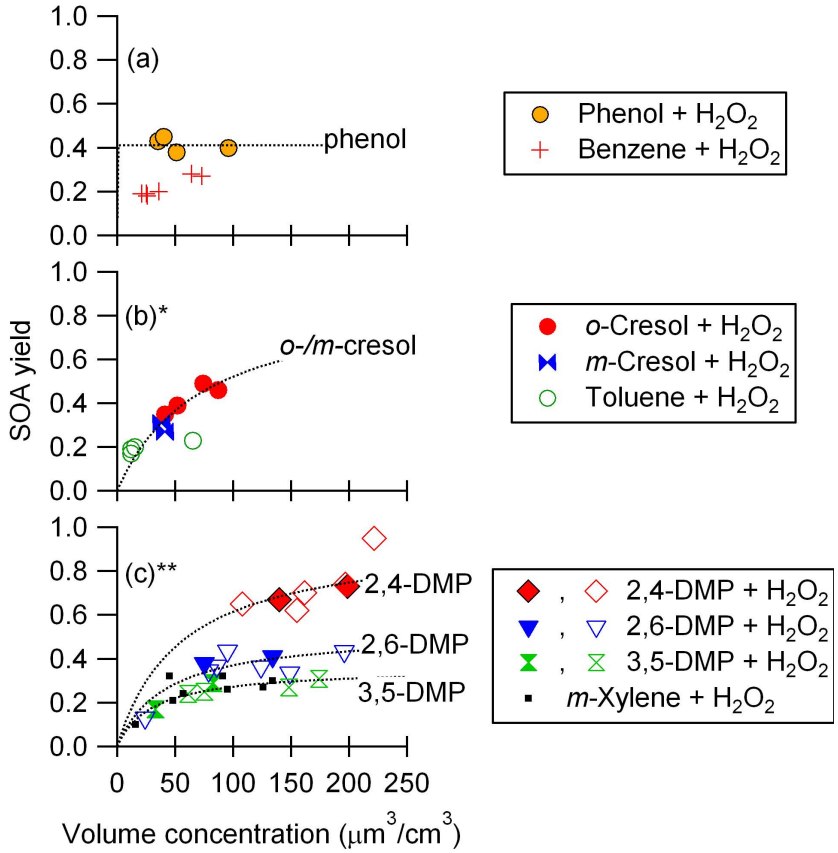

Fig. 1. SOA yield of benzene, toluene, *m*-xylene, and their phenolic compounds in the absence of NO_x (Dotted lines are one product model fit for phenolic compounds). * SOA yields from cresols isomers are combined. ** Open symbols are data acquired in CE-CERT mezzanine chamber.

ACPD
11, 2025–2055, 2011

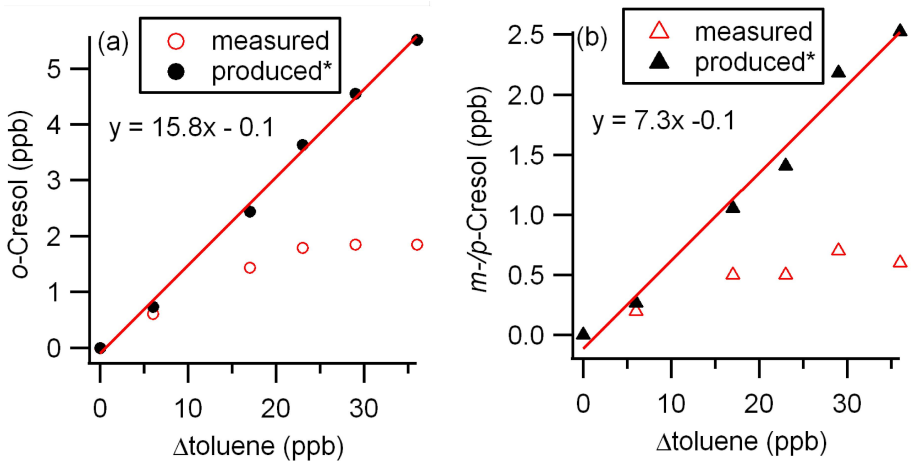

Fig. 2. Formation of cresols from OH reaction with toluene. * Measured cresol concentrations were corrected for secondary reaction.

ACPD
11, 2025–2055, 2011

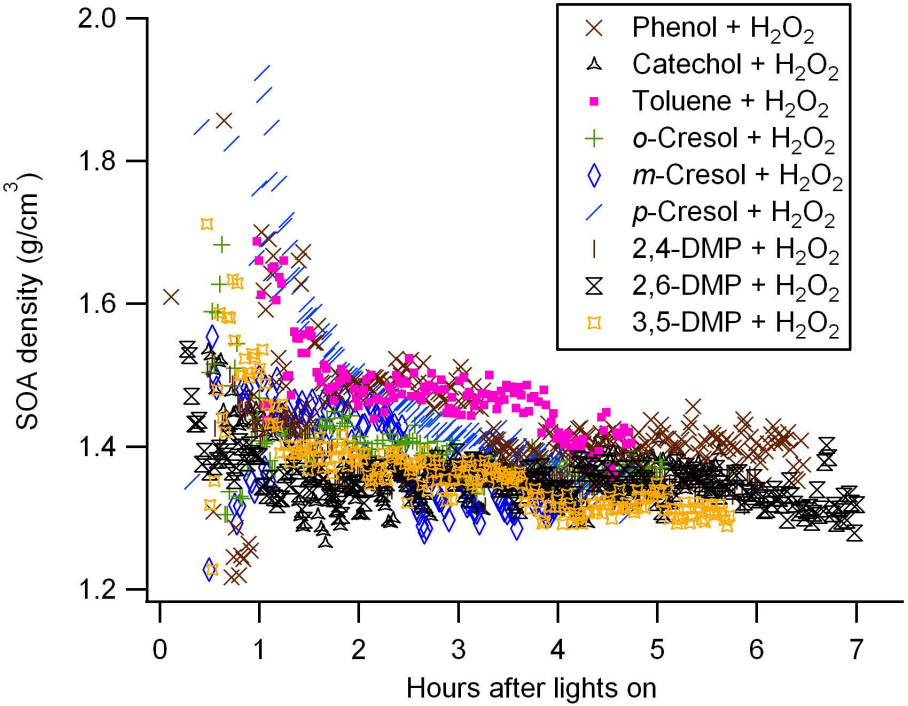

Fig. 3. Time series of the density of SOA formed from aromatic hydrocarbons and phenolic compounds.

ACPD
11, 2025–2055, 2011

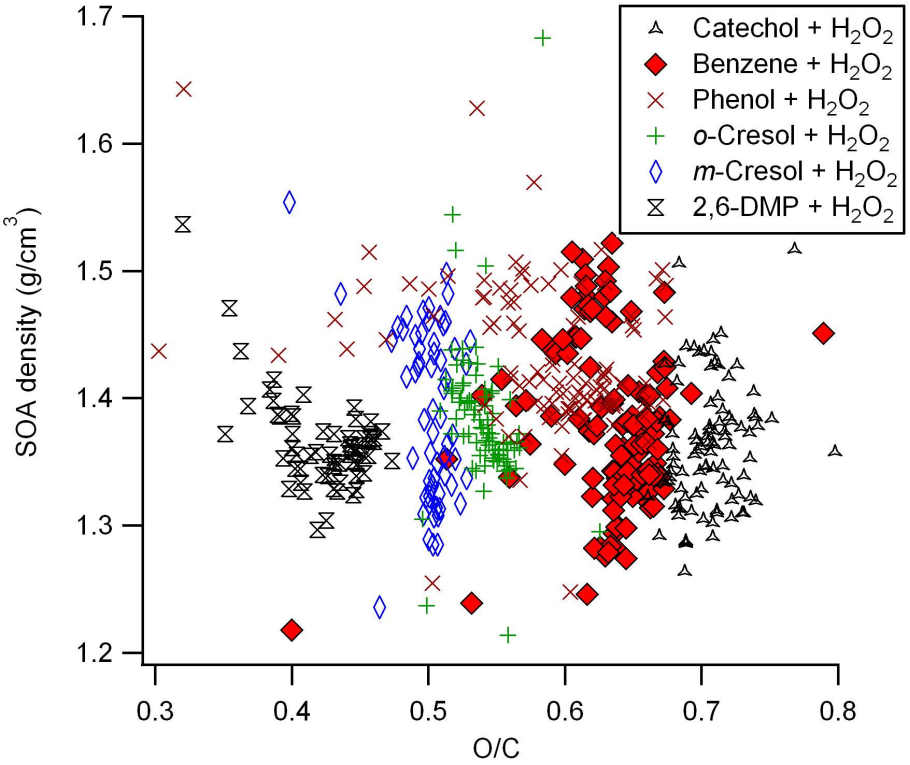

Fig. 4. The relationship between density and elemental compositions of SOA formed from aromatic hydrocarbons and phenolic compounds.

ACPD
11, 2025–2055, 2011

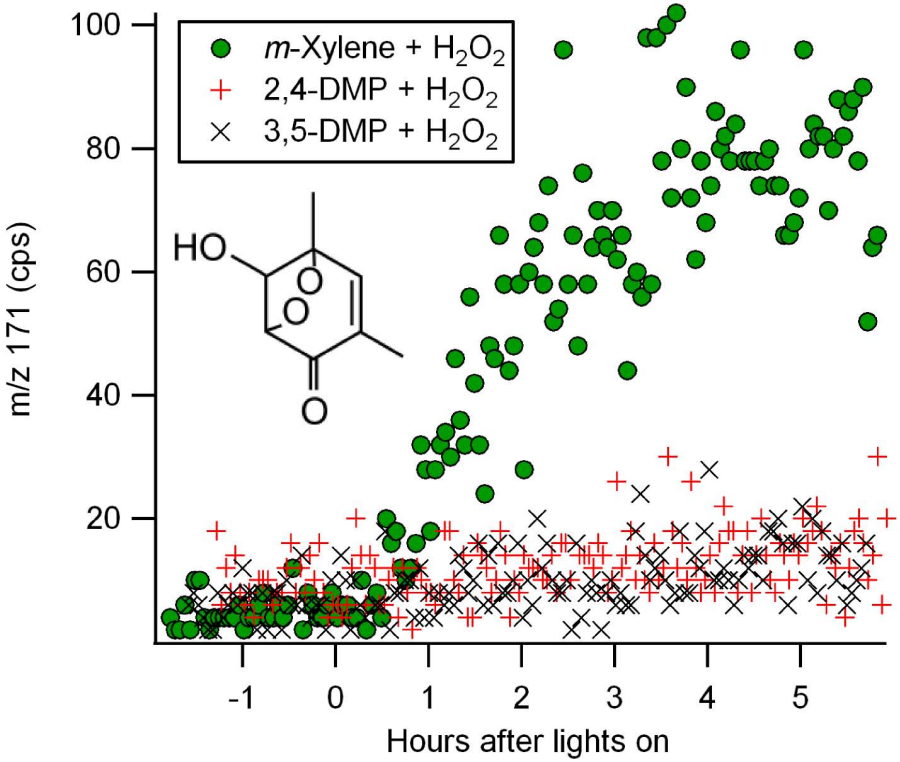

Fig. 5. Time series of *m/z* 171 observed by PTR-MS.

ACPD
11, 2025–2055, 2011

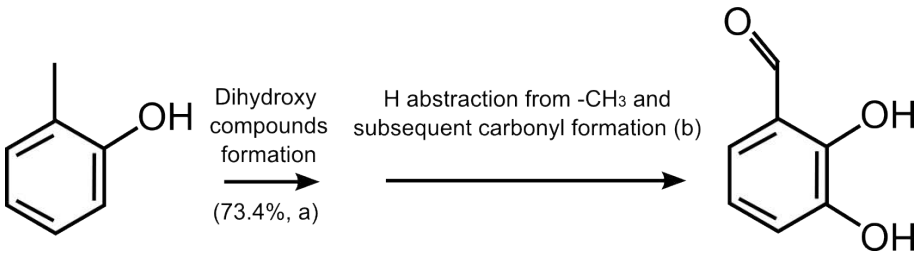

Fig. 6. Dihydroxybenzaldehydes formation from *o*-cresol. **(a)** Olariu et al. (2002), **(b)** the reaction mechanism of methylhydroperoxide is adapted from Atkinson et al. (2000).

ACPD
11, 2025–2055, 2011

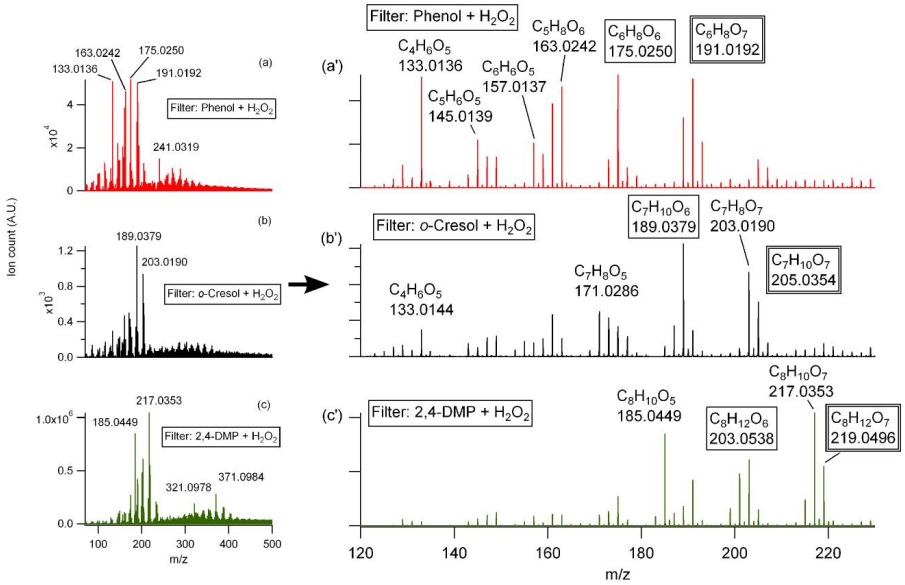

Fig. 7. ESI/APCI-ToF mass spectrums of SOA formed by OH reaction with phenolic compounds (the formulas inside boxes is consistent with bicyclic hydroperoxides formed from phenolic compounds and dihydroxy compounds).

ACPD
11, 2025–2055, 2011

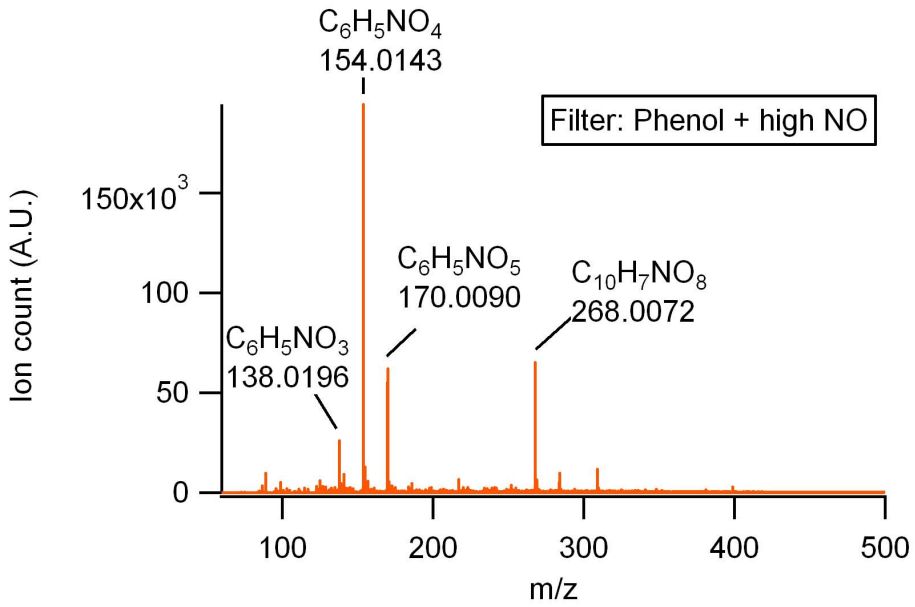

Fig. 8. ESI/APCI-ToF mass spectrum of SOA formed by OH reaction with phenol with the presence of excess NO.

ACPD
11, 2025–2055, 2011

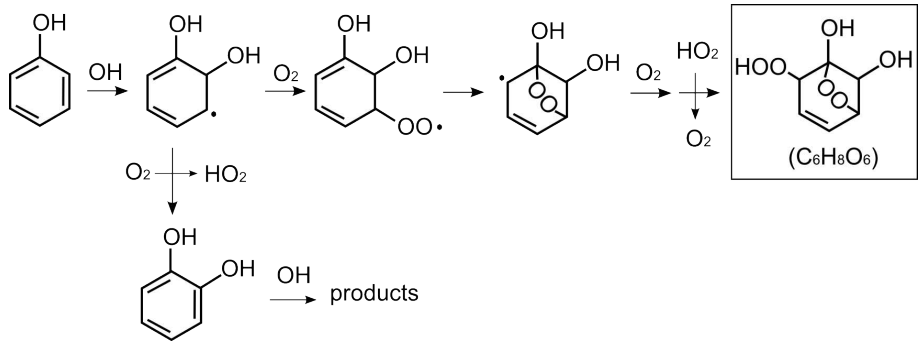

Fig. 9. Possible formation pathway of a bicyclic hydroperoxide ($C_6H_8O_6$) from OH reaction with phenol in the absence of NO_x.

ACPD
11, 2025–2055, 2011

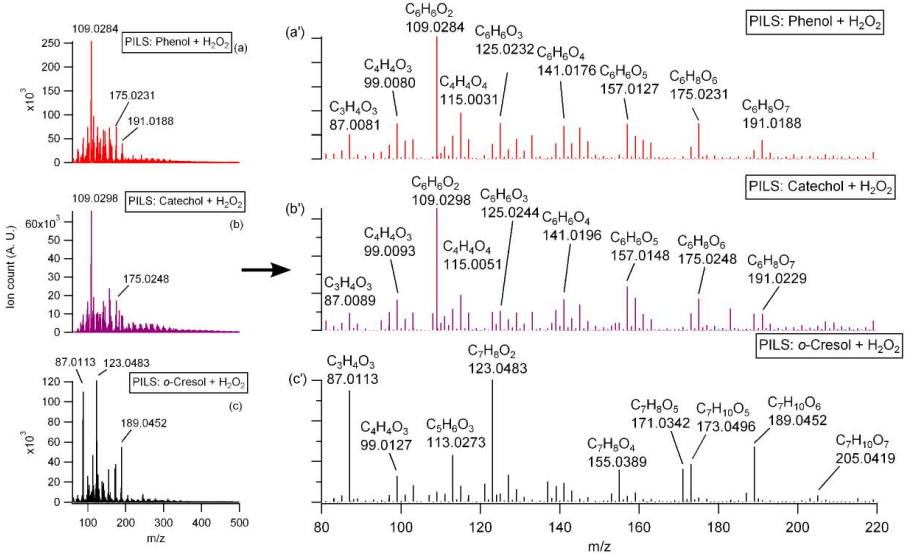

Fig. 10. PILS-ESI-ToF mass spectrums of SOA formed by OH reaction with phenolic compounds (the spectrum for phenol **(a)** and catechol **(b)** is taken when SOA concentration was highest. For *o*-cresol **(c)**, spectrum at highest $C_7H_8O_2$ is shown).

ACPD
11, 2025–2055, 2011